Power uprates
and plant life extension

CASL-U-2014-0352-000

Consortium for Advanced Simulation of LWRs

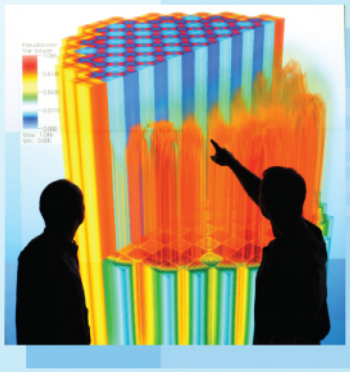

Engineering design
and analysis

Efficient Solution of the Simplified P_N Equations

Steven P. Hamilton, Thomas M. Evans
Oak Ridge National Laboratory

December 29, 2014

Science-enabling
high performance
computing

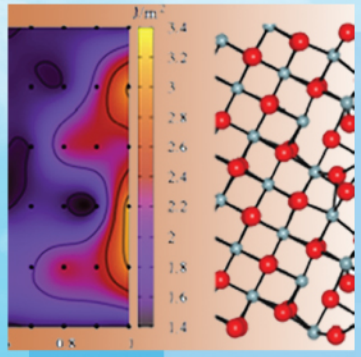

Fundamental science

Plant operational data

U.S. DEPARTMENT OF ENERGY | Nuclear Energy

Efficient solution of the simplified P_N equations[☆]

Steven P. Hamilton[a,1,*], Thomas M. Evans[a,1]

[a] *Oak Ridge National Laboratory, 1 Bethel Valley Rd., Oak Ridge, TN 37831 U.S.A.*

Abstract

In this paper we show new solver strategies for the multigroup SP_N equations for nuclear reactor analysis. By forming the complete matrix over space, moments, and energy, a robust set of solution strategies may be applied. Power iteration, shifted power iteration, Rayleigh quotient iteration, Arnoldi's method, and a generalized Davidson method, each using algebraic and physics-based multigrid preconditioners, have been compared on the C5G7 MOX test problem as well as an operational pressurized water reactor model. Our results show that the most efficient approach is the generalized Davidson method, which is 30–40 times faster than traditional power iteration and 6–10 times faster than Arnoldi's method.

Keywords: radiation transport, nuclear criticality, eigenvalue solvers

1. Introduction

Determining the power distribution across an entire reactor core is a critical component of the design and analysis of nuclear reactors. The power distribution can be determined by solving the Boltzmann neutron transport

[*]Corresponding Author

Email addresses: hamiltonsp@ornl.gov (Steven P. Hamilton), evanstm@ornlgov (Thomas M. Evans)

[1]Radiation Transport Group, Reactor and Nuclear Systems Division

CASL-U-2014-0352-000

equation; however, solution of consistent angular discretizations (such as discrete ordinates or spherical harmonics) for an entire reactor core in three dimensions can require substantional computational resources unlikely to be available to many analysts [1]. Thus, low-order approximations to the transport equation that can be solved at a sigificantly reduced computational cost are of great interest. Traditionally, this role has been filled by coarse mesh diffusion equations; however, such methods may be inadequate for advanced reactor designs [2]. The simplified P_N (SP_N) approximation offers the possibility of improved accuracy relative to diffusion by capturing some transport effects while still preserving many of the features that make diffusion solvers attractive. The SP_N approximation is a three-dimensional extension of the plane-geometry P_N equations. It was originally proposed by Gelbard [3], who applied heuristic arguments to justify the approximation. Since that time, both asymptotic [4–6] and variational [7] analyses have verified Gelbard's approach.

Because solvers for the SP_N equations have generally been used as replacements for ordinary diffusion solvers, code is commonly already available for the solution of diffusion equations. SP_N solvers have commonly been cast in such a way as to leverage existing diffusion machinery by iterating over the SP_N moment equations (each of which appears identical to a standard diffusion equation). In this study we pursue an alternate strategy, treating the SP_N equations as a single monolithic problem by constructing the full matrices involved. By explicitly storing these matrices, state of the art linear algebraic methods can be applied.

The rest of this paper is organized as follows. In § 2, a heuristic derivation of the SP_N equations from the 1-D P_N equations is presented. In § 3, a complete description of a finite volume discretization is introduced for SP_N orders up to seven, including discussion of the treatment of both vacuum and reflecting boundaries. In § 4, a brief overview of a wide range of eigenvalue solvers that can potentially be used to solve the k-eigenvalue form of the SP_N equations is given. Numerical results for several different eigenvalue solver and preconditioning approaches on two large test problems are presented in § 5, and some concluding remarks are given in § 6.

2. SP_N Equations

As mentioned in § 1, the SP_N method was originally based on heuristic arguments; however, several studies have performed both asymptotic and

variational analyses that have confirmed and justified the original *ad hoc* approximations. In this paper, we shall apply the heuristic approximation. The reader is directed towards Refs. [4–6] for more details on asymptotic derivations of the equations and Ref. [7] for a variational analysis of the SP_N equations. In addition, an excellent survey of the various formulations and derivations of the SP_N and related equations can be found in Ref. [8]. We begin our formulation of the SP_N equations by forming the planar, 1-D Legendre (P_N) equations in § 2.1. These equations will be used to motivate the SP_N equations that are given in § 2.2.

2.1. P_N Equations

We start with the steady-state, one-dimensional, eigenvalue-form of the linear Boltzmann transport equation,

$$\mu\frac{\partial\psi^g(x,\mu)}{\partial x}+\sigma^g(x)\psi^g(x,\mu)=\sum_{g'=1}^{N_g}\int_{4\pi}\sigma_{\mathrm{s}}^{gg'}(x,\hat{\mathbf{\Omega}}\cdot\hat{\mathbf{\Omega}}')\psi^{g'}(x,\mathbf{\Omega}')\,d\mathbf{\Omega}' + \frac{1}{k}\sum_{g'=1}^{N_g}\frac{\chi^g}{4\pi}\int_{4\pi}\nu\sigma_{\mathrm{f}}^{g'}(x)\,\psi^{g'}(x,\mathbf{\Omega}')\,d\mathbf{\Omega}'\,, \quad (1)$$

on the domain $x\in[x_\ell,x_h]$, with boundary conditions,

$$\psi^g(x,\mu_{\mathrm{in}})=\psi_{\mathrm{b}}^g(x,\mu_{\mathrm{in}})\,,\quad x\in\{x_\ell,x_h\} \quad (2)$$

where μ_{in} indicates the set of direction cosines that are incident on a given boundary. In Eqs. (1) and (2), energy is discretized using the multigroup approximation [9] where $g=1,\ldots,N_g$ is the energy group index. The quantities of interest are

$\psi^g(x,\mu)$	angular flux for group g in particles·cm^{-2}·sr^{-1},
$\psi_b^b(x,\mu_{\mathrm{in}})$	incident angular flux for group g on problem boundary,
$\sigma^g(x)$	total interaction cross section for group g in cm^{-1},
$\sigma_{\mathrm{s}}^{gg'}(x,\hat{\mathbf{\Omega}}\cdot\hat{\mathbf{\Omega}}')$	scattering cross section through angle $\mu_0=\hat{\mathbf{\Omega}}\cdot\hat{\mathbf{\Omega}}'$ from group $g'\rightarrow g$,
χ^g	the resulting fission spectrum in group g, and
$\nu\sigma_{\mathrm{f}}^{g'}(x)$	the number of neutrons produced per fission multiplied by the fission cross section for group g' in cm^{-1} .

The eigenvalue k is the ratio of neutron populations in subsequent fission generations; a value of unity defines a self-sustaining nuclear reaction. The work performed in this paper deals exclusively with the eigenvalue form of the Boltzmann equation. However, many of the methods presented in this paper can be applied equally well to the fixed-source SP_N equations that result from the linear Boltzmann equation with an external source defined on the right-hand side. The interested reader is directed to Appendix A for the SP_N equations defined with an external source.

The derivation of the P_N equations begins by expanding the angular flux and scattering cross section in Legendre polynomials (this requires spherical harmonics in two and three dimensions and non-Cartesian geometry):

$$\psi(\mu) = \sum_{n=0}^{N} \frac{2n+1}{4\pi} \phi_n P_n(\mu) \,, \tag{3}$$

$$\sigma_{\mathrm{s}}(\mu_0) = \sum_{m=0}^{N} \frac{2m+1}{4\pi} \sigma_{\mathrm{s}m} P_m(\mu_0) \,, \tag{4}$$

where $\mu_0 = \hat{\mathbf{\Omega}} \cdot \hat{\mathbf{\Omega}}'$. The addition theorem of spherical harmonics, simplified to 1-D planar geometry with azimuthal symmetry, is used in Eq. (4) to define the Legendre moment,

$$P_l(\hat{\mathbf{\Omega}} \cdot \hat{\mathbf{\Omega}}') = P_l(\mu_0) = P_l(\mu) P_l(\mu') \,. \tag{5}$$

The P_N equations are obtained by inserting the expansions in Eqs. (3) and (4) into Eq. (1), multiplying by $P_m(\mu)$, and integrating over μ. The recursion relation of Legendre polynomials is used to remove μP_n from the derivative term. Equation (5) is used in the scattering expansion to remove the μ_0 dependence. Orthogonality is used to remove all the remaining Legendre polynomials. The resulting system of equations is

$$\begin{aligned} \frac{\partial}{\partial x}\Big[\frac{n}{2n+1}\phi^g_{n-1} + \frac{n+1}{2n+1}\phi^g_{n+1}\Big] + \sum_{g'=1}^{N_g} (\sigma^g \delta_{gg'} - \sigma^{gg'}_{\mathrm{s}n})\phi^{g'}_n \\ = \frac{1}{k} \sum_{g'=1}^{N_g} \chi^g \nu\sigma^{g'}_{\mathrm{f}} \phi^{g'}_n \delta_{n0} \,, \quad n = 0, 1, 2, \ldots, N \,. \end{aligned} \tag{6}$$

Equation (6) defines a system of $N+1$ moment-equations with $N+2$ unknowns per energy group and spatial unknown; thus a closure relationship

is required to achieve a well-posed system. For steady-state problems, the common, and most straightforward, method for closing the equations is to set the highest order moment to zero, $\phi_{N+1} = 0$. This closure can be problematic in time-dependent applications of the P_N equations, potentially resulting in non-physical wave propagation speeds. In reactor applications, we are generally concerned with either eigenvalue or quasi-static applications of this model, and the simple closure is sufficient.

In this work, we consider both vacuum and reflective boundaries. For vacuum boundaries, we will employ the Marshak boundary conditions. The Marshak conditions approximately satisfy Eq. (2) at the boundary and are consistent with the P_N approximation. The generalized Marshak boundary condition is

$$2\pi \int_{\mu_{\text{in}}} P_i(\mu)\psi(\mu)\, d\mu = 0\,, \quad i = 1, 3, 5, \ldots, N\,. \tag{7}$$

Expanding ψ using Eq. (3) gives

$$2\pi \int_{\mu_{\text{in}}} P_i(\mu) \sum_{n=0}^{N} \frac{2n+1}{4\pi}\phi_n P_n(\mu)\, d\mu = 0\,, \quad i = 1, 3, 5, \ldots, N\,. \tag{8}$$

This form of the Marshak boundary conditions assumes no incoming current, which is appropriate for the eigenvalue problems we are studying here. Equation (8) yields $(N+1)/2$ fully coupled equations at each boundary and therefore fully closes the $N+1$ P_N equations given in Eq. (6).

As an example, we consider the P_3 equations. The Marshak conditions on the low boundary, i.e. $x = x_\ell$, are derived using

$$\begin{aligned} 2\pi \int_0^1 P_1(\mu) \sum_{n=0}^{3} \frac{2n+1}{4\pi}\phi_n P_n(\mu)\, d\mu = 0\,, \\ 2\pi \int_0^1 P_3(\mu) \sum_{n=0}^{3} \frac{2n+1}{4\pi}\phi_n P_n(\mu)\, d\mu = 0\,. \end{aligned} \tag{9}$$

Thus the P_3 Marshak boundary conditions are

$$\begin{aligned} \frac{1}{2}\phi_0 + \phi_1 + \frac{5}{8}\phi_2 = 0\,, \\ -\frac{1}{8}\phi_0 + \frac{5}{8}\phi_2 + \phi_3 = 0\,. \end{aligned} \tag{10}$$

As stated above, all of the moments are coupled in the boundary conditions.

Reflecting boundary conditions are more straightforward. The only condition that preserves symmetry in this case is to set all the odd moments to zero:

$$\phi_i = 0\,, \quad i = 1, 3, 5, \ldots, N\,. \tag{11}$$

This treatment also yields $(N+1)/2$ equations on each boundary and effectively closes the system. We note that both of these boundary treatments contain asymmetric components when N is even. Thus, we only consider odd sets of P_N (SP_N) equations.

2.2. SP_N Equations

We now turn our attention to the derivation of the SP_N equations. As mentioned previously, we will apply a heuristic approximation in this study; Refs. [4–7] give details on asymptotic derivations and a variational analysis of the equations.

In the notation that follows, we will employ the Einstein summation convention in which identical indices are implicitly summed over the range of 1 to 3,

$$a_i b_i = \sum_{i=1}^{3} a_i b_i = \mathbf{a} \cdot \mathbf{b}\,. \tag{12}$$

To form the SP_N equations, the following substitutions are made in Eq. (6):

- $\frac{\partial}{\partial x} \rightarrow \frac{\partial}{\partial x_i}$,
- convert odd moments to $\phi_{n,i}$, and
- use odd-order equations to remove odd moments from the even-order equations.

For boundary conditions, a similar process holds except that $\pm\frac{\partial}{\partial x} \rightarrow n_i \frac{\partial}{\partial x_i}$, where $\hat{\mathbf{n}} = n_i\mathbf{i} + n_j\mathbf{j} + n_k\mathbf{k}$ is the outward normal at a boundary surface, and $\mu \rightarrow |\hat{\mathbf{\Omega}} \cdot \hat{\mathbf{n}}|$. Applying this procedure to Eq. (6), the following system of

moment-equations is derived

$$\frac{\partial}{\partial x_i}\Big[\frac{n}{2n+1}\phi^g_{n-1,i}+\frac{n+1}{2n+1}\phi^g_{n+1,i}\Big]+\sum_{g'=1}^{N_g}(\sigma^g\delta_{gg'}-\sigma^{gg'}_{sn})\phi^{g'}_n = \frac{1}{k}\sum_{g'=1}^{N_g}\chi^g\nu\sigma^{g'}_{\rm f}\phi^{g'}_n\delta_{n0}\,,\quad n=0,2,4,\ldots,N\,, \tag{13}$$

$$\frac{\partial}{\partial x_i}\Big[\frac{n}{2n+1}\phi^g_{n-1}+\frac{n+1}{2n+1}\phi^g_{n+1}\Big]+\sum_{g'=1}^{N_g}(\sigma^g\delta_{gg'}-\sigma^{gg'}_{sn})\phi^{g'}_{n,i}=0\,,\quad n=1,3,5,\ldots,N\,. \tag{14}$$

Equations (13) and (14) are more easily expressed in operator notation over groups by defining

$$\Phi_n=\begin{pmatrix}\phi^0_n & \phi^1_n & \ldots & \phi^G_n\end{pmatrix}^T\,, \tag{15}$$

$$\Phi_{n,i}=\begin{pmatrix}\phi^0_{n,i} & \phi^1_{n,i} & \ldots & \phi^G_{n,i}\end{pmatrix}^T\,, \tag{16}$$

and

$$\mathbf{\Sigma}_n=\begin{pmatrix}(\sigma^0-\sigma^{00}_{sn}) & -\sigma^{01}_{sn} & \ldots & -\sigma^{0G}_{sn}\\ -\sigma^{10}_{sn} & (\sigma^1-\sigma^{11}_{sn}) & \ldots & -\sigma^{1G}_{sn}\\ \vdots & \vdots & \ddots & \vdots\\ -\sigma^{G0}_{sn} & -\sigma^{G1}_{sn} & \ldots & (\sigma^G-\sigma^{GG}_{sn})\end{pmatrix}. \tag{17}$$

Similarly, the fission matrix, $\mathbf{F}$, is defined

$$\mathbf{F}=\begin{pmatrix}\chi^0\nu\sigma^0_{\rm f} & \chi^0\nu\sigma^1_{\rm f} & \ldots & \chi^0\nu\sigma^G_{\rm f}\\ \chi^1\nu\sigma^0_{\rm f} & \chi^1\nu\sigma^1_{\rm f} & \ldots & \chi^1\nu\sigma^G_{\rm f}\\ \vdots & \vdots & \ddots & \vdots\\ \chi^G\nu\sigma^0_{\rm f} & \chi^G\nu\sigma^1_{\rm f} & \ldots & \chi^G\nu\sigma^G_{\rm f}\end{pmatrix}. \tag{18}$$

Thus, at any given spatial location, Φ_n and $\Phi_{n,i}$ are length N_g vectors, and $\mathbf{\Sigma}$ and $\mathbf{F}$ are $(N_g\times N_g)$ matrices. Using Eq. (14) to solve for the odd moments

gives

$$\Phi_{n,i} = -\boldsymbol{\Sigma}_n^{-1}\frac{\partial}{\partial x_i}\Big[\frac{n}{2n+1}\Phi_{n-1} + \frac{n+1}{2n+1}\Phi_{n+1}\Big] . \tag{19}$$

Substituting Eq. (19) into Eq. (13) yields

$$\begin{aligned} -\frac{\partial}{\partial x_i}\Bigg[&\frac{n}{2n+1}(\boldsymbol{\Sigma}_{n-1}^{-1})\frac{\partial}{\partial x_i}\Big(\frac{n-1}{2n-1}\Phi_{n-2} + \frac{n}{2n-1}\Phi_n\Big) + \\ &\frac{n+1}{2n+1}(\boldsymbol{\Sigma}_{n+1}^{-1})\frac{\partial}{\partial x_i}\Big(\frac{n+1}{2n+3}\Phi_n + \frac{n+2}{2n+3}\Phi_{n+2}\Big)\Bigg] + \\ &\boldsymbol{\Sigma}_n\Phi_n = \frac{1}{k}\mathbf{F}\Phi_n\delta_{n0} , \quad n = 0, 2, \ldots, N . \end{aligned} \tag{20}$$

Equation (20) defines the $(N+1)/2$ SP_N equations. These are a series of elliptic, second-order equations, each of which has a diffusion-like form.

Using Eq. (20), the four SP_7 equations are

$$\begin{aligned} -\nabla\cdot\frac{1}{3}\boldsymbol{\Sigma}_1^{-1}\nabla(\Phi_0 + 2\Phi_2) + \boldsymbol{\Sigma}_0\Phi_0 &= \frac{1}{k}\mathbf{F}\Phi_0 , \\ -\nabla\cdot\Big[\frac{2}{15}\boldsymbol{\Sigma}_1^{-1}\nabla(\Phi_0 + 2\Phi_2) + \frac{3}{35}\boldsymbol{\Sigma}_3^{-1}\nabla(3\Phi_2 + 4\Phi_4)\Big] + \boldsymbol{\Sigma}_2\Phi_2 &= 0 , \\ -\nabla\cdot\Big[\frac{4}{63}\boldsymbol{\Sigma}_3^{-1}\nabla(3\Phi_2 + 4\Phi_4) + \frac{5}{99}\boldsymbol{\Sigma}_5^{-1}\nabla(5\Phi_4 + 6\Phi_6)\Big] + \boldsymbol{\Sigma}_4\Phi_4 &= 0 , \\ -\nabla\cdot\Big[\frac{6}{143}\boldsymbol{\Sigma}_5^{-1}\nabla(5\Phi_4 + 6\Phi_6) + \frac{7}{195}\boldsymbol{\Sigma}_7^{-1}\nabla(7\Phi_6)\Big] + \boldsymbol{\Sigma}_6\Phi_6 &= 0 . \end{aligned} \tag{21}$$

A quick view of these equations reveals that certain linear combinations of moments appear together in the derivative terms. Performing the following variable transformation allows the gradient-term to operate on a single unknown in each moment equation,

$$\begin{aligned} \mathbb{U}_1 &= \Phi_0 + 2\Phi_2 , \\ \mathbb{U}_2 &= 3\Phi_2 + 4\Phi_4 , \\ \mathbb{U}_3 &= 5\Phi_4 + 6\Phi_6 , \\ \mathbb{U}_4 &= 7\Phi_6 . \end{aligned} \tag{22}$$

The inverse of this system is

$$\begin{aligned}
\Phi_0 &= \mathbb{U}_1 - \frac{2}{3}\mathbb{U}_2 + \frac{8}{15}\mathbb{U}_3 - \frac{16}{35}\mathbb{U}_4 \,, \\
\Phi_2 &= \frac{1}{3}\mathbb{U}_2 - \frac{4}{15}\mathbb{U}_3 + \frac{8}{35}\mathbb{U}_4 \,, \\
\Phi_4 &= \frac{1}{5}\mathbb{U}_3 - \frac{6}{35}\mathbb{U}_4 \,, \\
\Phi_6 &= \frac{1}{7}\mathbb{U}_4 \,.
\end{aligned} \tag{23}$$

Substituting Eqs. (22) and (23) into Eq. (21) and successively removing the lower order gradient terms from each equation results in the following concise form

$$-\nabla \cdot \mathbb{D}_n \nabla \mathbb{U}_n + \sum_{m=1}^{4} \mathbb{A}_{nm} \mathbb{U}_m = \frac{1}{k} \sum_{m=1}^{4} \mathbb{F}_{nm} \mathbb{U}_m \,, \quad n = 1, 2, 3, 4 \,. \tag{24}$$

The effective diffusion coefficients in the multigroup problem are the $(N_g \times N_g)$ matrices defined by

$$\mathbb{D}_1 = \frac{1}{3}\boldsymbol{\Sigma}_1^{-1} \,, \quad \mathbb{D}_2 = \frac{1}{7}\boldsymbol{\Sigma}_3^{-1} \,, \quad \mathbb{D}_3 = \frac{1}{11}\boldsymbol{\Sigma}_5^{-1} \,, \quad \mathbb{D}_4 = \frac{1}{15}\boldsymbol{\Sigma}_7^{-1} \,. \tag{25}$$

Defining the coefficient matrices

$$\mathbf{c}^{(1)} = \begin{pmatrix} 1 & -\frac{2}{3} & \frac{8}{15} & -\frac{16}{35} \\ -\frac{2}{3} & \frac{4}{9} & -\frac{16}{45} & \frac{32}{105} \\ \frac{8}{15} & -\frac{16}{45} & \frac{64}{225} & -\frac{128}{525} \\ -\frac{16}{35} & \frac{32}{105} & -\frac{128}{525} & \frac{256}{1225} \end{pmatrix} , \tag{26}$$

$$\mathbf{c}^{(2)} = \begin{pmatrix} 0 & 0 & 0 & 0 \\ 0 & \frac{5}{9} & -\frac{4}{9} & \frac{8}{24} \\ 0 & -\frac{4}{9} & \frac{16}{45} & -\frac{32}{105} \\ 0 & \frac{32}{105} & -\frac{32}{105} & \frac{64}{245} \end{pmatrix} , \tag{27}$$

$$\mathbf{c}^{(3)} = \begin{pmatrix} 0 & 0 & 0 & 0 \\ 0 & 0 & 0 & 0 \\ 0 & 0 & \frac{9}{25} & -\frac{54}{175} \\ 0 & 0 & -\frac{45}{175} & \frac{324}{1225} \end{pmatrix} , \tag{28}$$

$$\mathbf{c}^{(4)} = \begin{pmatrix} 0 & 0 & 0 & 0 \\ 0 & 0 & 0 & 0 \\ 0 & 0 & 0 & 0 \\ 0 & 0 & 0 & \frac{13}{49} \end{pmatrix} , \tag{29}$$

we can write the blocks of the matrices $\mathbb{A}$ and $\mathbb{F}$ as

$$\mathbb{A}_{nm} = \sum_{i=1}^{4} \mathbf{c}_{nm}^{(i)} \mathbf{\Sigma}_i \, , \tag{30}$$

and

$$\mathbb{F}_{nm} = \mathbf{c}_{nm}^{(1)} \mathbf{F} \, . \tag{31}$$

Equation (24) is the form of the SP_N equations that we will use in the remainder of this paper. Setting $\Phi_2 = \Phi_4 = \Phi_6 = 0$ gives the SP_1 equation,

$$-\nabla \cdot \frac{1}{3} \mathbf{\Sigma}_1^{-1} \nabla \Phi_0 + \mathbf{\Sigma}_0 \Phi_0 = \frac{1}{k} \mathbf{F} \Phi_0 \, . \tag{32}$$

This equation is identical in form to the standard multigroup diffusion equation; the only difference between the SP_1 and multigroup diffusion equations

is that the off-diagonal terms in $\mathbf{\Sigma}_1$ are retained in the SP_1 equation. Equivalently, the SP_3 equations are obtained by setting $\Phi_4 = \Phi_6 = 0$, and the SP_5 equations result from setting $\Phi_6 = 0$.

The P_7 Marshak boundary conditions are obtained by carrying out the integrations in Eq. (8) to produce

$$\begin{aligned}
\frac{1}{2}\Phi_0 + \Phi_1 + \frac{5}{8}\Phi_2 - \frac{3}{16}\Phi_4 + \frac{13}{128}\Phi_6 = 0\,, \\
-\frac{1}{8}\Phi_0 + \frac{5}{8}\Phi_2 + \Phi_3 + \frac{81}{128}\Phi_4 - \frac{13}{64}\Phi_6 = 0\,, \\
\frac{1}{16}\Phi_0 - \frac{25}{128}\Phi_2 + \frac{81}{128}\Phi_4 + \Phi_5 + \frac{325}{512}\Phi_6 = 0\,, \\
-\frac{5}{128}\Phi_0 + \frac{7}{64}\Phi_2 - \frac{105}{512}\Phi_4 + \frac{325}{512}\Phi_6 + \Phi_7 = 0\,.
\end{aligned} \tag{33}$$

These equations are converted into SP_N boundary conditions using the same procedure that was used to form Eq. (24). Eq. (19) is used to remove the odd moments ($\{\Phi_{1,i}, \Phi_{3,i}, \Phi_{5,i}, \Phi_{7,i}\}$) from Eq. (33), and the SP_N boundary approximation,

$$\pm\frac{\partial}{\partial x} \rightarrow \hat{\mathbf{n}} \cdot \nabla\,,$$

is used for the gradient terms. Finally, Eqs. (22) and (23) are used to transform the resulting system into $\{\mathbb{U}_1 \ldots \mathbb{U}_4\}$. Application of these steps gives the SP_N Marshak boundary conditions,

$$-\hat{\mathbf{n}} \cdot \mathbb{J}_n + \sum_{m=1}^{4} \mathbb{B}_{nm}\mathbb{U}_m = 0\,. \tag{34}$$

The moments are coupled on the boundary through the $\mathbb{B}$ matrix, each block of which is an $(N_g \times N_g)$ multiple of the identity matrix, i.e.,

$$\mathbb{B}_{nm} = \mathbf{b}_{nm}\mathbf{I}_{N_g}\,, \tag{35}$$

where $\mathbf{b}_{nm}$ is the (n, m) entry in the coefficient matrix

$$\mathbf{b} = \begin{pmatrix} \frac{1}{2} & -\frac{1}{8} & \frac{1}{16} & -\frac{5}{128} \\ -\frac{1}{8} & \frac{7}{24} & -\frac{41}{384} & \frac{1}{16} \\ \frac{1}{16} & -\frac{41}{384} & \frac{407}{1920} & -\frac{233}{2560} \\ -\frac{5}{128} & \frac{1}{16} & -\frac{233}{2560} & \frac{3023}{17920} \end{pmatrix}\,. \tag{36}$$

The current, $\mathbb{J}_n$, is a length N_g vector; it is related to the flux by Fick's Law,

$$\mathbb{J}_n = -\mathbb{D}_n \nabla \mathbb{U}_n \, . \tag{37}$$

The P_N boundary conditions for reflecting surfaces are given in Eq. (11). Applying the SP_N approximation to these boundary conditions yields

$$\nabla \mathbb{U}_n = 0 \, , \quad n = 1, 2, 3, 4 \, . \tag{38}$$

This implies that $\hat{\mathbf{n}} \cdot \mathbb{J} = 0$ on the boundaries.

In summary, the SP_N equations are given in Eq. (24) and yield $(N+1)/2$ second-order equations. The SP_N Marshak boundary conditions are given in Eq. (34) for vacuum boundaries. Equation (38) gives reflecting boundary conditions. Each boundary condition yields $(N+1)/2$ first-order (Robin) conditions that closes the system of SP_N equations. Although not relevant to the discussion of eigenvalue problems, a discussion of isotropic source boundary conditions is provided in Appendix A.

We note that this is not the only formation of the SP_N equations. References [4], [10], and [11] derive a canonical form of the SP_N equations that is based on the equivalence of the one-dimensional, planar P_N and S_{N+1} (discrete ordinates) equations. Starting from the S_{N+1} equations and using even-odd parity expansions of the angular flux, a system of SP_N equations is derived that is algebraically identical to the SP_N equations presented here. The principal advantage of such an approach is that the fluxes are uncoupled at the boundary.

3. Discrete SP_N Equations

Here we describe the formulation of the discrete SP_N operator using finite-volume discretization on regular, Cartesian grids. Because there is nothing particularly novel about the finite-volume approach employed here, this material is presented briefly with the goal of understanding the nature and structure of the resulting discrete SP_N operator that is required to describe the solution methods in § 4.

The general form for the SP_N equations is given in Eq. (24); Marshak boundary conditions are defined in Eq. (34); reflecting boundary conditions are given by Eq. (38). Applying Fick's Law [Eq. (37)] to Eq. (24) gives

$$\nabla \cdot \mathbb{J}_n + \sum_{m=1}^{4} \mathbb{A}_{nm} \mathbb{U}_m = \mathbb{Q}_n \, , \quad n = 1, 2, 3, 4 \, . \tag{39}$$

Because there is no spatial coupling in the fission source, we have represented it in the term $\mathbb{Q}_n$. The finite-volume discretization is defined on a 3-D, orthogonal Cartesian grid with logical dimensions $0 < i, j, k < N_{i,j,k}$, where $N_{i,j,k}$ is the number of computational cells in i, j, or k, respectively. The finite-volume form of the equations is derived by integrating Eq. (39) over a cell volume and applying the divergence theorem. These operations give the following balance equation in cell (i, j, k),

$$(\mathbb{J}_{n,i+1/2} - \mathbb{J}_{n,i-1/2})\Delta_j\Delta_k + (\mathbb{J}_{n,j+1/2} - \mathbb{J}_{n,j-1/2})\Delta_i\Delta_k + (\mathbb{J}_{n,k+1/2} - \mathbb{J}_{n,k-1/2})\Delta_i\Delta_j + \sum_{m=1}^{4} \mathbb{A}_{nm,ijk}\mathbb{U}_{m,ijk}V_{ijk} = \mathbb{Q}_{n,ijk}V_{ijk} \,. \quad (40)$$

Here, we have written the face-edge currents with suppressed subscripts as follows:

$$\mathbb{J}_{n,i\pm1/2\,jk} \rightarrow \mathbb{J}_{n,i\pm1/2} \,, \quad \mathbb{J}_{n,i\,j\pm1/2\,k} \rightarrow \mathbb{J}_{n,j\pm1/2} \,, \quad \mathbb{J}_{n,ij\,k\pm1/2} \rightarrow \mathbb{J}_{n,k\pm1/2} \,.$$

The same convention will be applied to all face-edge quantities.

Applying second-order differencing to Fick's Law, Eq. (37), in each direction for the plus/minus faces of the computational cell gives

$$\begin{aligned} \mathbb{J}_{n,l+1/2} &= -\frac{1}{\Delta_{l+1/2}}\mathbb{D}_{n,l+1/2}(\mathbb{U}_{n,l+1} - \mathbb{U}_{n,l}) \,, \\ \mathbb{J}_{n,l-1/2} &= -\frac{1}{\Delta_{l-1/2}}\mathbb{D}_{n,l-1/2}(\mathbb{U}_{n,l} - \mathbb{U}_{n,l-1}) \,, \end{aligned} \quad (41)$$

for $l = i, j, k$, and $\Delta_{l\pm1/2} = \frac{1}{2}(\Delta_l + \Delta_{l\pm1})$. We note here that the true, physical current is the first moment of the angular flux and is not equivalent to $\mathbb{J}_n$. Using Eq. (41), the balance equation (40) can be written in terms of the unknowns $\mathbb{U}$; however, the cell-edge diffusion coefficients must be defined. To make the method consistent, the moments and their first derivatives must be continuous at inter-cell boundaries. This condition implies that the effective currents, $\mathbb{J}$, are continuous across cell boundaries, i.e.,

$$\begin{aligned} \mathbb{J}^-_{n,l+1/2} &= \mathbb{J}^+_{n,l+1/2} \,, \\ -2\mathbb{D}_{n,l}\frac{\mathbb{U}_{n,l+1/2} - \mathbb{U}_{n,l}}{\Delta_l} &= -2\mathbb{D}_{n,l+1}\frac{\mathbb{U}_{n,l+1} - \mathbb{U}_{n,l+1/2}}{\Delta_{l+1}} \,, \end{aligned} \quad (42)$$

and

$$\begin{aligned} \mathbb{J}^{-}_{n,l-1/2} &= \mathbb{J}^{+}_{n,l-1/2} \,, \\ -2\mathbb{D}_{n,l-1}\frac{\mathbb{U}_{n,l-1/2}-\mathbb{U}_{n,l-1}}{\Delta_{l-1}} &= -2\mathbb{D}_{n,l}\frac{\mathbb{U}_{n,l}-\mathbb{U}_{n,l-1/2}}{\Delta_{l}} \,. \end{aligned} \tag{43}$$

Solving for the $(N_g \times N_g)$ cell-edge unknowns, $\{\mathbb{U}_{n,l\pm1/2}\}$, substituting these values back into $\mathbb{J}^{+}_{n,l\pm1/2}$, and setting the resulting equation equal to Eq. (41) gives the cell-edge diffusion coefficients that preserve continuity of current at the cell interfaces,

$$\begin{aligned} \mathbb{D}_{n,l+1/2} &= 2\Delta_{l+1/2}\mathbb{D}_{n,l+1}(\Delta_l\mathbb{D}_{n,l+1}+\Delta_{l+1}\mathbb{D}_{n,l})^{-1}\mathbb{D}_{n,l} \,, \\ \mathbb{D}_{n,l-1/2} &= 2\Delta_{l-1/2}\mathbb{D}_{n,l}(\Delta_l\mathbb{D}_{n,l-1}+\Delta_{l-1}\mathbb{D}_{n,l})^{-1}\mathbb{D}_{n,l-1} \,. \end{aligned} \tag{44}$$

Inserting Eq. (44) into Eq. (41) gives the internal cell-edge currents that can be used in in Eq. (40). Grouping unknowns yields

$$\begin{aligned} &-\mathbb{C}^{+}_{n,i}\mathbb{U}_{n,i+1\,jk}-\mathbb{C}^{-}_{n,i}\mathbb{U}_{n,i-1\,jk}-\mathbb{C}^{+}_{n,j}\mathbb{U}_{n,i\,j+1\,k}-\mathbb{C}^{-}_{n,j}\mathbb{U}_{n,i\,j-1\,k}- \\ &\quad \mathbb{C}^{+}_{n,k}\mathbb{U}_{n,ij\,k+1}-\mathbb{C}^{-}_{n,k}\mathbb{U}_{n,ij\,k-1}+\sum_{m=1}^{4}\big[\mathbb{A}_{nm,ijk}+(\mathbb{C}^{+}_{m,i}+\mathbb{C}^{-}_{m,i} \\ &\quad +\mathbb{C}^{+}_{m,j}+\mathbb{C}^{-}_{m,j}+\mathbb{C}^{+}_{m,k}+\mathbb{C}^{-}_{m,k})\delta_{nm}\big]\mathbb{U}_{m,ijk}=\mathbb{Q}_{n,ijk} \,, \\ &\qquad\qquad\qquad\qquad\qquad\qquad\qquad\qquad\qquad\qquad n=1,2,3,4 \,, \end{aligned} \tag{45}$$

where

$$\begin{aligned} \mathbb{C}^{+}_{n,l} &= \frac{2}{\Delta_l}\mathbb{D}_{n,l+1}(\Delta_l\mathbb{D}_{n,l+1}+\Delta_{l+1}\mathbb{D}_{n,l})^{-1}\mathbb{D}_{n,l} \,, \\ \mathbb{C}^{-}_{n,l} &= \frac{2}{\Delta_l}\mathbb{D}_{n,l}(\Delta_l\mathbb{D}_{n,l-1}+\Delta_{l-1}\mathbb{D}_{n,l})^{-1}\mathbb{D}_{n,l-1} \,. \end{aligned} \tag{46}$$

The fission source is

$$\mathbb{Q}_{n,ijk}=\frac{1}{k}\sum_{m=1}^{4}\mathbb{F}_{nm,ijk}\mathbb{U}_{m,ijk} \,. \tag{47}$$

The Marshak boundary conditions given in Eq. (34) couple all of the moments at the problem boundaries. In finite-volume discretizations of standard diffusion operators, these unknowns can be algebraically eliminated from the system of equations. However, the moment coupling in SP_N prevents this

simplification and imposes the introduction of cell-edge unknowns. The cell-edge currents that are inserted into Eq. (40) on low and high boundaries are

$$\mathbb{J}_{n,1/2} = -\frac{2}{\Delta_1}\mathbb{D}_{n,1}(\mathbb{U}_{n,1} - \mathbb{U}_{n,1/2}) \,, \tag{48}$$

$$\mathbb{J}_{n,L+1/2} = -\frac{2}{\Delta_L}\mathbb{D}_{n,L}(\mathbb{U}_{n,L+1/2} - \mathbb{U}_{n,L}) \,. \tag{49}$$

In order to close the system of equations for the added unknowns $\{\mathbb{U}_{n,1/2}, \mathbb{U}_{n,L}\}$, we use Eq. (34) with cell-edge currents defined by Eqs. (48) and (49) on the low and high boundaries, respectively. The resulting equations close the system

$$\sum_{m=1}^{4}\Big(\mathbb{B}_{nm} + \frac{2}{\Delta_1}\mathbb{D}_{n,1}\delta_{nm}\Big)\mathbb{U}_{m,1/2} - \frac{2}{\Delta_1}\mathbb{D}_{n,1}\mathbb{U}_{n,1} = 0 \,, \tag{50}$$

$$\sum_{m=1}^{4}\Big(\mathbb{B}_{nm} + \frac{2}{\Delta_L}\mathbb{D}_{n,L}\delta_{nm}\Big)\mathbb{U}_{m,L+1/2} - \frac{2}{\Delta_L}\mathbb{D}_{n,L}\mathbb{U}_{n,L} = 0 \,. \tag{51}$$

Likewise, reflecting boundary conditions are imposed with

$$\mathbb{J}_{n,1/2} = 0 \,, \tag{52}$$

$$\mathbb{J}_{n,L+1/2} = 0 \,, \tag{53}$$

which get used in Eq. (40) at reflecting boundaries. No additional unknowns are required at reflecting boundary faces.

To review, Eqs. (48) and (49) define the cell-edge currents that are inserted into the balance equation (40) on low and high boundary faces that have vacuum boundaries. Equations (50) and (51) provide the additional equations needed to close the system for the added unknowns on those faces. On reflecting faces no additional equations are required and the cell-edge net currents are zero.

Equation (45), with the appropriate boundary conditions defined by Eqs. (48)–(51), can be written in operator form as a generalized eigenvalue problem,

$$\mathbf{A}\mathbf{u} = \frac{1}{k}\mathbf{B}\mathbf{u} \,. \tag{54}$$

Here, we explicitly form the matrices $\mathbf{A}$ and $\mathbf{B}$. Forming the matrix once at the beginning of a solve reduces the runtime because the $(N_g \times N_g)$ matrix

inverses required to calculate the $\mathbb{C}_n^{\pm}$ need only be performed once per solve. Furthermore, any branching logic needed at problem boundaries is codified in the matrix. Explicit formulation of the matrix system also enables the use of algebraic preconditioners, the benefits of which are shown in § 5. Finally, adjoint calculations are easily defined by simply taking the transpose of formulated matrices. These advantages are at least partially offset by the increased memory requirements associated with storing the matrix.

The choice to construct the SP_N equations as a monolithic system should be contrasted with approaches generally taken in the literature, which involve solving the SP_N equations using a Gauss–Seidel approach over the moment equations and possibly energy [7, 10, 12]. Indeed, it was observed in Ref. [12] through both Fourier analysis and numerical experiments that the monoenergetic form of the SP_N equations considered in this study (denoted the "composite" formulation by Zhang, Ragusa, and Morel) experience significant degradation in iterative convergence as the SP_N order is increased. Despite this fact, this method was observed to be the favored approach for problems with high scattering ratios and relatively low SP_N orders. Considering that Gauss–Seidel over energy is known to exhibit poor iterative performance for problems with significant upscattering [13, 14], use of a Gauss–Seidel approach over *both* moments and energy is certain to result in slow convergence. Thus, avoiding the use of Gauss–Seidel iterations altogether in favor of solution approaches targeted at the entire matrix at once is an attractive option.

The multigroup SP_N equations have dimension $N_g \times N_m \times N_c$, where $N_m = (N+1)/2$ is the number of moment equations; N_c is the number of spatial cells; and, as mentioned previously, N_g is the number of energy groups. The solution vector $\mathbf{u}$ can be ordered in multiple ways; however, the ordering that minimizes the bandwidth of the matrix is to order $\mathbf{u}$ in groups-moments-cells,

$$\mathbf{u} = \begin{pmatrix} u_0 & u_1 & \dots & u_{m-1} & u_m & u_{m+1} & \dots & u_M \end{pmatrix}^T , \tag{55}$$

with

$$m = g + N_g(n + cN_m) , \tag{56}$$

where g is the group, n is the moment equation, and c is the cell. Consider an example SP_3 matrix that results from a $2 \times 2 \times 4$ grid with 4 groups. With all reflecting boundary conditions, the total number of unknowns is 128. Alternatively, vacuum boundary conditions must be coupled over all equations

as indicated by Eq. (34); thus the size of the matrix will be augmented by $N_b \times N_g \times N_m$ unknowns, where N_b is the number of boundary cells over all faces. The sparsity plot for a $2 \times 2 \times 4$ grid with vacuum boundary conditions on four faces is shown in Fig. 1.

One feature of the SP_N equations is that, for many problems of interest, scattering moments above P_1 are not required to attain sufficient accuracy. Thus, all $\mathbf{\Sigma}_n$ matrices with $n > 1$ will simply be diagonal matrices. Also, there is relatively little coupling from low to high energy groups in most physical regimes, which yields $\mathbf{\Sigma}_n$ matrices that are predominately lower-triangular. A sparsity plot of a representative $\mathbf{\Sigma}_n$ matrix with 56 energy groups is shown in Fig. 2. It should be noted that while the monoenergetic SP_N equations are symmetric, the multigroup equations are nonsymmetric and therefore require the use of both eigensolvers and linear solvers intended for use with nonsymmetric systems.

Because the SP_N equations do not represent a consistent discretization of the neutron transport equation in general (only in limited asymptotic regimes is this true), it should be emphasized that SP_N should not be used to resolve the sharp material boundaries that would be present in a fully heterogeneous model of a nuclear reactor core. Instead, typical use of the SP_N equations for reactor analysis involves first homogenizing portions of the reactor into homogeneous subregions. This process is identical to the approach used for core-wide diffusion calculations [15]. The basis for this homogenization may be either full reactor assemblies [16] or individual fuel pins [2]. For the numerical results presented in § 5, we use pin cells as the basis for homogenization. Unlike the approach taken in Ref. [2], no discontinuity or homogenization factors are used in the present study. Because the SP_N equations in 2D and 3D do not limit to the solution of the Boltzmann equation, the maximum accuracy is achieved for some finite value of N and beyond that point the error will increase. It has been observed that the majority of the benefit of using SP_N rather than diffusion is achieved at low angular orders; therefore, SP_N solvers typically focus on SP_3 or SP_5 calculations [2, 7, 16].

4. Eigenvalue Solvers

Although we are currently considering the solution of the SP_N k-eigenvalue problem, the form of the eigenvalue problem given by Eq. (54) is the same as for other transport discretizations, even if the linear operators themselves are different. Therefore, much of the following discussion is equally applica-

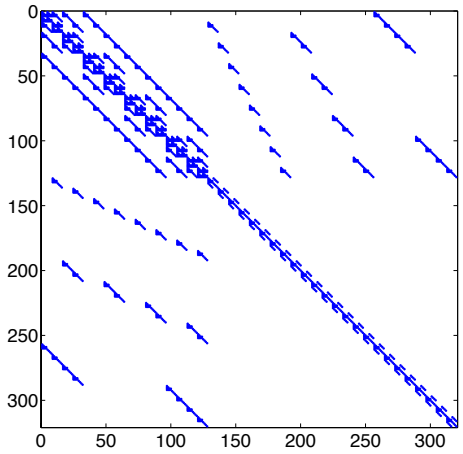

(a) Full matrix.

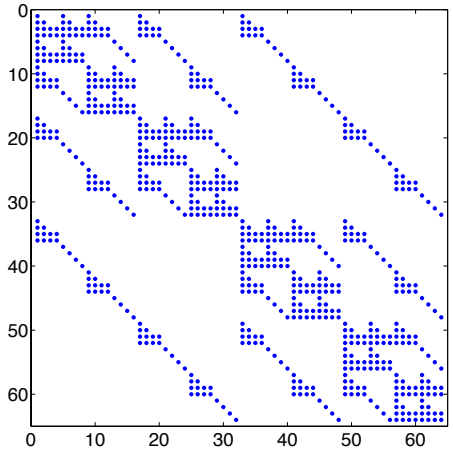

(b) Close-up of the leading 64×64 block of the full matrix.

Figure 1: SP_3 matrix sparsity pattern for a $2 \times 2 \times 4$ spatial grid and 4 energy groups.

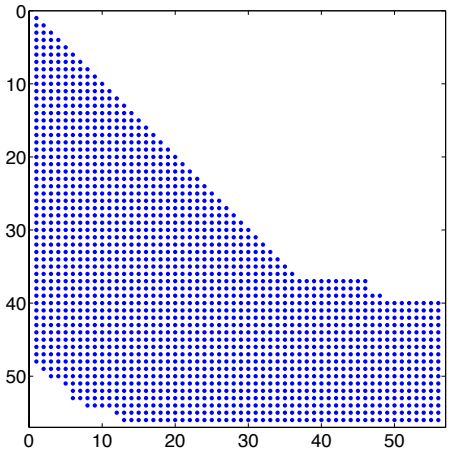

Figure 2: Sparsity of 56 group $\mathbf{\Sigma}_n$ matrix.

ble to not only the SP_N equations, but also other angular approximations (e.g. discrete ordinates or diffusion). Several eigenvalue solvers have been proposed in the literature for the k-eigenvalue problem. Many approaches are based on converting the generalized eigenvalue problem of Eq. (54) to the equivalent standard eigenvalue problem

$$\mathbf{A}^{-1}\mathbf{B}\mathbf{u} = k\mathbf{u}\,. \tag{57}$$

Such a conversion is possible because the matrix $\mathbf{A}$ is guaranteed to be non-singular [17]. In practice, factorizations of $\mathbf{A}$ will be too dense to store explicitly, but the matrix-vector product $\mathbf{y} = \mathbf{A}^{-1}\mathbf{B}\mathbf{v}$ can be computed by first performing the product $\mathbf{z} = \mathbf{B}\mathbf{v}$, followed by solving the linear system $\mathbf{A}\mathbf{y} = \mathbf{z}$. The simplest and perhaps most widely used approach is to use power iteration (PI) applied to the operator $\mathbf{A}^{-1}\mathbf{B}$. Convergence to the dominant eigenvalue is guaranteed under very general conditions [18], but rates of convergence (dictated by the dominance ratio $\rho \equiv \frac{k_2}{k_1}$, where k_1 and k_2 are the largest and second largest eigenvalues, respectively) may be prohibitively slow for many problems of interest. The rate of convergence of PI can be improved by first applying a shift to Eq. (54) before inverting, i.e.,

$$\left(\mathbf{A} - \mu\mathbf{B}\right)^{-1}\mathbf{B}\mathbf{u} = \bar{k}\mathbf{u}\,, \tag{58}$$

where μ is a fixed approximation to the inverse of the dominant eigenvalue [19]. It can easily be shown that the eigenvalue of the shifted system, $\bar{k}$, is

related to the eigenvalue of the original system by

$$k = \frac{\bar{k}}{1 + \mu\bar{k}} , \tag{59}$$

and that the dominance ratio is given by $\rho_{\text{shift}} = \left(\frac{k_2}{k_1}\right)\left(\frac{k_1 - 1/\mu}{k_2 - 1/\mu}\right)$, which can be significantly smaller than the dominance ratio of the original problem for $\mu \approx \frac{1}{k_1}$. Shifted power iteration faces two primary difficulties. First, improper selection of the shift will cause the method to converge to an incorrect eigenvalue. Second, solving linear systems involving the shifted matrix $(\mathbf{A} - \mu\mathbf{B})$ may be significantly more difficult than linear systems involving the unshifted matrix. This increased difficulty arises because of a clustering of the spectrum of the shifted matrix around 0 when μ is close to a true eigenvalue.

A natural extension of the shifted PI is to use the current eigenvalue estimate as a shift rather than using a fixed value. This results in the Rayleigh quotient iteration (RQI) algorithm:

$$\mathbf{u}^{(m+1)} = \left(\mathbf{A} - \lambda^{(m)}\mathbf{B}\right)^{-1} \mathbf{B}\mathbf{u}^{(m)} , \tag{60}$$

$$\lambda^{(m+1)} = \frac{\langle \mathbf{u}^{(m+1)}, \mathbf{A}\mathbf{u}^{(m+1)} \rangle}{\langle \mathbf{u}^{(m+1)}, \mathbf{B}\mathbf{u}^{(m+1)} \rangle} , \tag{61}$$

where m is the iteration index and $\langle \cdot, \cdot \rangle$ indicates an inner product. The primary advantage of RQI is that convergence is quadratic and thus very few iterations will generally be required. The difficulties associated with shifted PI, however, are made even worse. Convergence to the dominant eigenvalue is not guaranteed, regardless of the choice of initial shift, and the linear systems that must be solved are not only more difficult than the unshifted systems, but increase in difficulty as the algorithm progresses because $(\mathbf{A} - \lambda\mathbf{B})$ approaches a singular matrix as λ approaches the true eigenvalue. RQI has only recently begun to attract attention for radiation transport problems [20–22].

The methods discussed so far are all fixed-point methods, i.e., the next estimate of the solution depends only on the estimate immediately preceding it. An alternative to fixed-point iterations is subspace eigenvalue solvers in which information from several previous vectors is used to generate the next approximate solution. The vast majority of subspace solvers are built on two basic principles: extracting an approximate solution from a given subspace and adding an additional vector (or vectors) to the current subspace. In the

solution extraction phase, an estimate of the desired eigenvector is obtained as a linear combination of the subspace basis vectors. The process is almost invariably achieved through a Rayleigh–Ritz procedure, solving the projected eigenvalue problem

$$\mathbf{V^T A V y} = \lambda \mathbf{V^T B V y} \,, \tag{62}$$

or for a standard eigenvalue problem [i.e., for solving Eq. (57)]

$$\mathbf{V^T A^{-1} B V y} = k\mathbf{y} \,, \tag{63}$$

where $\mathbf{V}$ contains a set of (typically orthogonal) basis vectors for the current subspace. For an appropriate selection of $\mathbf{V}$, the eigenvalues of the projected problem will closely approximate the eigenvalues of the original system, and the vectors $\mathbf{Vy}$ will approximate the corresponding eigenvectors. The approximate eigenvalues and eigenvectors obtained from the Rayleigh–Ritz procedure are generally referred to as Ritz values and Ritz vectors, respectively. In the case of symmetric matrices, it can be shown that the Ritz values and vectors satisfy certain optimality conditions. In the nonsymmetric case, no such optimality conditions apply, although the Rayleigh–Ritz procedure is still the basis for many eigensolvers [23].

The method of subspace expansion is what distinguishes the majority of subspace eigensolvers. In the Arnoldi method [24], the subspace is taken to be the Krylov subspace corresponding to the operator $\mathbf{A}^{-1}\mathbf{B}$. Thus, each iteration requires the operator action $\mathbf{y} = \mathbf{A}^{-1}\mathbf{Bx}$, just as with PI. Unlike PI, however, convergence of Arnoldi's method is not dictated by the dominance ratio, and so the number of iterations required to converge is likely to be significantly smaller. The Arnoldi method has gained attention in the transport literature in recent years and has become the staple of some production codes [25, 26].

Another subspace eigensolver is the Davidson method [27]. The central idea behind subspace expansion in the Davidson method is that at iteration m, given an approximate eigenvalue, $\lambda^{(m)}$, and corresponding eigenvector, $\mathbf{u}^{(m)}$, one should seek a correction, $\mathbf{t}^{(m)}$, such that the eigenvalue correction equation given by

$$\mathbf{A}(\mathbf{u}^{(m)} + \mathbf{t}^{(m)}) = \lambda^{(m)}\mathbf{B}(\mathbf{u}^{(m)} + \mathbf{t}^{(m)}) \,, \tag{64}$$

is satisfied. Rearranging this equation yields

$$(\mathbf{A} - \lambda^{(m)}\mathbf{B})\mathbf{t}^{(m)} = -(\mathbf{A} - \lambda^{(m)}\mathbf{B})\mathbf{u}^{(m)} \equiv -\mathbf{r}^{(m)} \,, \tag{65}$$

where $\mathbf{r}^{(m)}$ is the residual of the eigenvalue problem. This equation implies that a linear system involving the matrix $(\mathbf{A} - \lambda^{(m)}\mathbf{B})$ must be solved at each iteration. This is likely to incur a significant computational expense, suggesting the use of a preconditioner, $\mathbf{M}$, that approximates $(\mathbf{A} - \lambda^{(m)}\mathbf{B})$, leading to the Davidson correction equation

$$\mathbf{M}\mathbf{t}^{(m)} = -\mathbf{r}^{(m)} \,. \tag{66}$$

Although the original Davidson method was targeted at the symmetric standard eigenvalue problem, later work extended the idea to the generalized eigenvalue problem [28] and to nonsymmetric matrices [29]. The Davidson method has one extremely appealing feature for the k-eigenvalue problem: because it solves the generalized eigenvalue problem directly, it is not necessary to solve any linear system involving the full problem operator; only a preconditioner approximating the solution of a linear system is required. Despite this attractive feature, use of the Davidson method for transport problems has only very recently appeared in the literature [21, 30, 31].

Although it will not be considered further in this study, another subspace solver that has garnered much attention in the mathematics community in recent years is the Jacobi-Davidson method [32]. The Jacobi–Davidson correction equation is given by

$$\left(\mathbf{I} - \mathbf{u}\mathbf{u}^T\right)\left(\mathbf{A} - \lambda^{(m)}\mathbf{B}\right)\left(\mathbf{I} - \mathbf{u}\mathbf{u}^T\right)\mathbf{t}^{(m)} = -\mathbf{r}^{(m)} \,, \tag{67}$$

where the projection operator $\left(\mathbf{I} - \mathbf{u}\mathbf{u}^T\right)$ forces the update to be orthogonal to the current solution estimate and prevents stagnation of the method.

A classification of the eigenvalue solvers discussed here is given in Table 1 based on the linear system that each method is required to solve. This list is not intended to be exhaustive, as several other subspace eigenvalue solvers appear in the mathematics literature. Additionally, eigensolvers based on optimization strategies or general nonlinear solvers exist (the latter case was studied in Refs. [33, 34] for the k-eigenvalue problem).

The idea of preconditioning for eigensolvers involving a conversion to a standard eigenvalue problem is straightforward: a preconditioner is applied to accelerate the convergence of the solution of the relevant linear system of equations only and therefore does not directly influence the rate of convergence of the eigensolver (though clearly it influences the efficiency of the overall approach). Preconditioning for eigenvalue solvers operating directly on a generalized eigenvalue problem (e.g., Davidson-style methods) is not

Table 1: Classification of eigensolvers by linear system solution required

	Solver Type	
Linear System Matrix	Fixed Point	Subspace
$\mathbf{M}$	–	Davidson
$\mathbf{A}$	Power Iteration	Arnoldi
$\mathbf{A} - \mu\mathbf{B}$	Shifted Power Iteration	Shift-and-Invert Arnoldi
$\mathbf{A} - \lambda^{(m)}\mathbf{B}$	Rayleigh Quotient It.	Jacobi-Davidson*

*The Jacobi-Davidson correction equation includes additional projection operators.

understood as well. Preconditioning in these cases has a direct impact on the rate of convergence of the eigensolver. Davidson's original method focused solely on the use of diagonal preconditioning (a natural choice because the matrices under consideration were strongly diagonally dominant), though subsequent studies considered more general preconditioners [35, 36]. Generally speaking, the preconditioner, $\mathbf{M}$, should approximate the matrix $(\mathbf{A} - \lambda^{(m)}\mathbf{B})$. Care must be taken, however, because stagnation can occur if $\mathbf{M}$ too closely approximates $(\mathbf{A} - \lambda^{(m)}\mathbf{B})$. The reason for this can easily be seen from Eq. (65), which admits $\mathbf{t}^{(m)} = \mathbf{u}^{(m)}$ as a solution. Thus, the vector proposed for addition to the current subspace is already contained in the subspace, and no further progress toward a solution can be made. One possible remedy for this stagnation, proposed by Olsen [37], is to force the subspace expansion to be orthogonal to the current iterate. The downside to this approach is that two applications of the preconditioner are required at each iteration, rather than only a single application in the standard Davidson method.

One preconditioning approach that obviates the stagnation issue is to have $\mathbf{M}$ approximate $(\mathbf{A} - \mu\mathbf{B})$ for a fixed value of μ. In fact, if the smallest magnitude eigenvalue is being sought, it may be sufficient to have $\mathbf{M}$ approximate $\mathbf{A}$. In the limiting case where $\mathbf{M} = \mathbf{A}$, the subspace constructed by the Davidson method is the Krylov subspace corresponding to $\mathbf{A}^{-1}\mathbf{B}$ and is thus equivalent (in exact arithmetic) to the Arnoldi method. Using the Arnoldi method in this case, however, requires $\mathbf{A}^{-1}$ to be applied to high accuracy to maintain the structure of the subspace. For problems where direct factorization of $\mathbf{A}$ is not practical, this can impose a significant computational burden. The Davidson method, on the other hand, explicitly computes the

residual at each iteration and thus is not constrained by the accuracy to which the linear solves are performed. In this respect, the Davidson method with $\mathbf{M} \approx \mathbf{A}$ can be viewed as an inexact Arnoldi approach. There is a cost associated with the freedom to perform inexact solves: storage of additional basis vectors and additional orthogonalization work must be done because the subspace has no structure for the subspace for the Davidson solver to exploit.

5. Computational Results

To test the relative merits of the various solvers described in the previous section, each solver is tested on two different test problems: a modified version of the 3-D C5G7 MOX benchmark and a model of the initial criticality at Unit 1 of the Watts Bar Nuclear Plant (WBN1). The discretization of the SP_N equations described in § 3 has been implemented in the Denovo radiation transport code [38]. The solvers under consideration are PI, shifted PI, RQI, the Arnoldi method, and the Davidson method.

For each eigensolver, three different preconditioners are considered. First is a thresholded incomplete LU factorization (ILUT) with a drop tolerance of 10^{-2} provided by the IFPACK package [39]. No domain overlap is included, so in parallel calculations each processor only performs a factorization of the portion of the matrix local to that processor. The second preconditioner is an algebraic multigrid (AMG) preconditioner provided by the ML package [40]. Default settings for a "DD" problem type are used (see reference for full description of these settings). The final preconditioner is a multigrid in energy (MGE) approach, similar to the strategies developed in Refs. [41] and [21]. The smoother for all MGE cases consists of three iterations of ILU-preconditioned BiCGStab. The linear solver for all cases is right-preconditioned GMRES as provided by Belos [42]. In the case of MGE, a flexible GMRES implementation is used [43]. The eigensolver implementations for the Arnoldi and Davidson approaches are provided by the Anasazi package of Trilinos [44]. An important point to note is that all of the solvers except for Davidson use a preconditioner to accelerate the solution of a linear system; the Davidson solver uses the preconditioner directly for expansion of the subspace and does not make use of a linear solver.

5.1. C5G7 MOX Benchmark

The first problem under consideration is a slight modification of the 3-D C5G7 MOX benchmark problem. We base our model on the original benchmark specification described in Ref. [45] rather than the more commonly modeled variant described in Ref. [46]. The only difference in the problem specifications is the height of the fuel assemblies (the original problem used a fuel height of 385.56 cm while the more recent specification reduced this height to 42.84 cm). We choose the original specification because it more closely resembles a typical PWR geometry and is more challenging from a solver convergence perspective. The problem geometry consists of a 4×4 checkerboard array of fuel assemblies, each containing a 17×17 square array of pins (264 fuel pins, 25 guide tubes) with a pitch of 1.26 cm. Half of the assemblies contain 4.0% enriched UO_2 fuel, and the remaining half contain several different enrichments of MOX fuel. The height of the fuel is 385.56 cm, and a 21.42 cm reflector surrounds the assembly radially and axially. Symmetry reduces the problem to only a single octant of the full problem. For each pin cell, the benchmark specifies two materials: a homogenized fuel material and a moderator. In this study, we choose to instead use the heterogeneous pin specifications given in Ref. [47] and use the XSDRN module of the SCALE package [48] to generate pin-homogenized 23-group cross sections for the SP_N solver. This process preserves the pertinent features of the benchmark problem while closely following a typical reactor physics workflow. The problem is solved using an SP_3 angular expansion, a 2×2 mesh per pin cell radially and a 2.5 cm mesh height axially. The problem was run in parallel on 81 processing cores with a 9×9 spatial decomposition in the x-y plane. The computed dominant eigenvalue was between 1.161599 and 1.161600 for all solvers, values that were consistent with the specified stopping criteria of 10^{-6} in the L_2 norm of the residual. The dominance ratio was estimated to be approximately 0.978

Table 2 shows the convergence behavior and run time performance for each eigensolver/preconditioner combination on the C5G7 problem. The first significant trend to notice is the behavior of different preconditioners for the same eigensolver. With PI, the fastest time to solution is achieved with the ILUT preconditioner despite the fact that it results in far more total linear iterations than the other preconditioners; this is because the time required to apply the ILUT preconditioner is far less than the cost of applying either the AMG or MGE preconditioners. For shifted PI (for this problem a shift of $\mu = 0.8$ is used) and RQI, the situation is entirely different: the MGE

preconditioner results in the smallest computational time. The reason for this difference is that the linear systems that must be solved in shifted PI and RQI are much more difficult than the linear systems encountered by PI; the stronger preconditioning offered by the multigrid preconditioners results in less degradation of the iterative performance of the linear solver when moving to the shifted linear systems and therefore a faster time to solution. Arnoldi shows a similar trend to PI with respect to preconditioning, which is not a surprising result considering the same linear system is solved in both methods. Finally, the Davidson method displays very similar time to solution for all three preconditioning approaches despite widely varying iteration counts. This robustness with respect to preconditioner selection is a very attractive feature of the Davidson approach.

The second significant feature to note in this study is the relative solve times between the different eigensolvers. Shifted PI results in significantly fewer eigenvalue iterations compared to PI, although the run time is only slightly less than PI (or even greater than PI, depending on the preconditioner selection) because of the increased difficulty of the linear system that must be solved. RQI results in a very small number of eigenvalue iterations due to the quadratic convergence of the solver and shows a significant reduction in runtime relative to PI or shifted PI. Arnoldi's method produces an iteration count virtually equivalent to shifted PI, however the total iteration count and time to solution are much lower than with shifted PI. Arnoldi's method and RQI result in very similar linear iteration counts and solution times. Finally, the generalized Davidson method produces a much lower time to solution than any of the other solvers, solving the problem approximately five times faster than the next best approach. The reason for this small time to solution is that the eigenvalue iteration counts are not dramatically larger than those using the other solvers, but each iteration is much less expensive because no system of linear equations must be solved.

5.2. Watts Bar Nuclear 1

The second test problem is a model of the initial criticality at WBN1. The reactor core consists of 193 fuel assemblies containing three different enrichments of fresh UO_2 fuel. Each assembly consists of a 17×17 array of pins with 264 fuel pins, 24 guide tubes, and a central instrumentation tube. The pins are located on a 1.26 cm square pitch array, and a 0.08 cm gap is present between each assembly. The active height of the fuel is 365.76 cm, with a 16 cm helium-filled plenum above the fuel. Eight spacer grids, top

Table 2: Convergence behavior for the C5G7 MOX problem

Eigensolver	**Prec.**	**Eigenvalue Iterations**	**Total Linear Iterations**	**Setup (min)**	**Solve (min)**
PI	ILUT	418	14366	3.4	137.9
	AMG	415	5551	0.8	199.7
	MGE	418	2347	0.8	289.3
Shifted PI	ILUT	24	5615	3.5	288.5
	AMG	24	2258	1.0	107.3
	MGE	24	666	0.8	83.7
RQI	ILUT	4	1744	3.2	89.9
	AMG	4	526	0.8	28.7
	MGE	4	156	0.9	21.2
Arnoldi	ILUT	23	1786	3.4	27.6
	AMG	23	728	0.8	27.1
	MGE	23	304	0.9	51.1
Davidson	ILUT	263	–	3.4	5.1
	AMG	96	–	0.8	4.2
	MGE	29	–	0.9	4.4

and bottom assembly nozzles, and top and bottom core plates are included in the model. Hot zero power conditions at a uniform temperature of 565K are modeled. Reactivity control is achieved through a combination of 1285 ppm soluble boron, pyrex rods inserted into select guide tube locations, and one partially inserted control rod bank. Further material and geometric details of the problem can be found in Ref. [49]. The problem is solved using 256 processing cores.

For this problem, the same five eigensolvers are used, but only the AMG and MGE preconditioners are used. The use of an ILUT preconditioner resulted in excessively large iteration counts and run times; therefore, this approach was excluded from this comparison. The failure of an ILU-style preconditioner on this number of processors is not particularly surprising, as such preconditioners are well known to exhibit poor parallel scaling performance [50]. Variants of incomplete factorizations aimed at improving parallel performance exist, but investigation into such approaches is well outside the scope of this work. All solvers computed a dominant eigenvalue between 1.000759 and 1.000761, consistent with the stopping criteria of 10^{-6} and quite close to the measured critical state of the reactor. The dominance ratio of the system was estimated to be approximately 0.987.

Table 3 shows the convergence behavior and timings for the various solvers on the WBN1 problem. The general trends for the different solvers are very similar to those for the C5G7 problem. PI, as expected, displays the worst performance in both iteration count and run time. The use of shifted PI (with a shift of $\mu = 0.95$) offers a moderate reduction in run time, and RQI improves performance even further. The Arnoldi method outperforms any of the fixed-point solvers, although its performance is not dramatically different from RQI. The Davidson solver once again appears as the clear-cut winner, outperforming all of the other solvers by around an order of magnitude in run time. In terms of preconditioning, the AMG approach seems to offer the most favorable performance in terms of time to solution for most solvers. Only in the case of RQI does the MGE preconditioner offer an advantage.

6. Conclusions

The SP_N equations offer an attractive alternative to standard diffusion approximations to the neutron transport equation. Because the equations account for transport effects that cannot be captured by diffusion alone, SP_N is more appropriate for analysis of advanced reactor designs. At the same

Table 3: Convergence behavior for the WBN1 problem

Eigensolver	Prec.	Eigenvalue Iterations	Total Linear Iterations	Setup (min)	Solve (min)
PI	AMG	523	10572	0.7	353.1
	MGE	523	4919	0.7	851.5
Shifted PI	AMG	16	2647	0.7	161.5
	MGE	16	1319	0.7	224.7
RQI	AMG	3	765	0.7	125.6
	MGE	3	435	0.8	103.1
Arnoldi	AMG	43	2118	0.7	85.4
	MGE	43	901	0.7	109.0
Davidson	AMG	201	–	0.8	8.5
	MGE	76	–	0.7	10.1

time, the SP_N equations retain a diffusion-like structure that is appealing from the standpoint of numerical solvers, avoiding the high computational cost associated with solving fully consistent discretizations of the transport equation.

An in-depth discussion of the derivation, discretization, and solution of the k-eigenvalue form of the SP_N equations has been presented in this paper. The solution strategies presented in this work are unique in that they focus on the full construction of problem matrices, in constrast with typical approaches that solve sequentially over the moment equations to facilitate the use of existing diffusion solver capabilities. The use of various eigensolvers on light water reactor problems has been investigated. In particular, it has been shown that the use of a generalized Davidson eigenvalue solver offers a particularly efficient solution approach. This efficiency is because of the fact that the generalized Davidson solver directly solves the generalized eigenvalue problem rather than first converting it to a standard eigenvalue problem, eliminating the need to solve linear systems of equations involving the full problem matrix at each iteration.

Acknowledgements

Work for this paper was supported by Oak Ridge National Laboratory, which is managed and operated by UT-Batelle, LLC, for the U.S. Department of Energy under Contract No. DEAC05-00OR22725. This research was supported by the Consortium for Advanced Simulation of Light Water Reactors (www.casl.gov), an Energy Innovation Hub (http://www.energy.gov/hubs) for Modeling and Simulation of Nuclear Reactors under U.S. Department of Energy Contract No. DE-AC05-00OR22725.

Appendix A. Fixed-Source SP_N Equations

In § 2 we derived the eigenvalue form of the SP_N equations. However, many applications require solutions to problems that contain a fixed source. Because the fixed-source form of the SP_N equations has the same left-hand side as the eigenvalue form, many of the solution strategies discussed in § 4 can be applied to fixed-source problems. Therefore, we present a brief derivation of the SP_N equations for fixed-source problems.

The steady-state, one-dimensional linear Boltzmann equation for problems with an external source is

$$\mu\frac{\partial\psi^g(x,\mu)}{\partial x}+\sigma^g(x)\psi^g(x,\mu)= \sum_{g'=1}^{N_g}\int_{4\pi}\sigma_{\rm s}^{gg'}(x,\hat{\mathbf{\Omega}}\cdot\hat{\mathbf{\Omega}}')\psi^{g'}(x,\mathbf{\Omega}')\,d\mathbf{\Omega}'+\frac{q^g(x,\mu)}{2\pi}\,. \quad \text{(A.1)}$$

For simplicity, we only consider isotropic sources; thus,

$$\frac{q^g(x,\mu)}{2\pi}\rightarrow\frac{q^g(x)}{4\pi}\,. \quad \text{(A.2)}$$

The only difference between the fixed-source form and Eq. (1) is that the right-hand side now contains an external source, q, instead of a fission source and eigenvalue.

Following the identical procedure on Eq. (A.1) as that performed in § 2 on Eq. (1), the fixed-source SP_N equations are defined,

$$-\nabla\cdot\mathbb{D}_n\nabla\mathbb{U}_n+\sum_{m=1}^{4}\mathbb{A}_{nm}\mathbb{U}_m=\mathbb{Q}_{\text{ext}\,n}\,,\quad n=1,2,3,4\,. \quad \text{(A.3)}$$

The right-hand side source is

$$\mathbb{Q}_{\text{ext}\,n} = \mathbf{c}_{1n}^{(1)}\mathbf{q}\,, \tag{A.4}$$

where $\mathbf{c}^{(1)}$ is defined in Eq. (26), and

$$\mathbf{q} = \begin{pmatrix} q^0 & q^1 & \dots & q^G \end{pmatrix}^T\,. \tag{A.5}$$

The reflecting and vacuum boundary conditions for this system of equations are given in Eqs. (34) and (38). For fixed-source problems, we must also consider the case of boundary fluxes. The generalized Marshak boundary condition for a boundary flux, ψ_{b}, is

$$2\pi \int_{\mu_{\text{in}}} P_i(\mu)\psi(\mu)\,d\mu = 2\pi \int_{\mu_{\text{in}}} P_i(\mu)\psi_{\text{b}}(\mu)\,d\mu\,, \quad i = 1, 3, 5, \dots, N\,. \tag{A.6}$$

Assuming an isotropic flux on the boundary,

$$\psi_{\text{b}}(\mu) = \frac{\phi_{\text{b}}}{4\pi}\,, \tag{A.7}$$

and performing the SP_N approximation gives the following equation on the problem boundary,

$$-\hat{\mathbf{n}}\cdot\mathbb{J}_n + \sum_{m=1}^{4}\mathbb{B}_{nm}\mathbb{U}_m = \mathbb{S}_n\,. \tag{A.8}$$

This equation is identical to Eq. (34) with the exception of the presence of a boundary source on the right-hand side. The boundary source is defined,

$$\mathbb{S}_n = \mathbf{b}_{1n}\mathbf{s}\,, \tag{A.9}$$

where $\mathbf{b}_{1n}$ is given in Eq. (36), and

$$\mathbf{s} = \begin{pmatrix} \phi_{\text{b}}^0 & \phi_{\text{b}}^1 & \dots & \phi_{\text{b}}^G \end{pmatrix}^T\,. \tag{A.10}$$

References

[1] J. Jarrell, T. Evans, G. Davidson, A. Godfrey, Full core reactor analysis: Running Denovo on Jaguar, Nuclear Science and Engineering 175 (3) (2013) 283–291.

[2] T. Kozlowski, Y. Xu, T. J. Downar, D. Lee, Cell homogenization method for pin-by-pin neutron transport calculations, Nuclear Science and Engineering 169 (1) (2011) 1–18.

[3] E. Gelbard, Application of the spherical harmonics to reactor problems, Tech. Rep. WAPD-BT-20, Westinghouse Atomic Power Department (Sept 1960).

[4] E. W. Larsen, J. E. Morel, J. M. McGhee, Asymptotic Derivation of the Multigroup P1 and Simplified PN Equations with Anisotropic Scattering, Nuclear Science and Engineering 123 (1996) 328–342.

[5] E. W. Larsen, G. Thömmes, A. Klar, M. Sead, T. Götz, Simplified PN Approximations to the Equations of Radiative Heat Transfer and Applications, Journal of Computational Physics 183 (2) (2002) 652–675.

[6] M. Frank, A. Klar, E. W. Larsen, S. Yasuda, Time-dependent simplified PN approximation to the equations of radiative transfer, Journal of Computational Physics 226 (2) (2007) 2289–2305.

[7] P. S. Brantley, E. W. Larsen, The Simplified P3 Approximation, Nuclear Science and Engineering 134 (2000) 1–21.

[8] R. G. McClarren, Theoretical aspects of the simplified p_n equations, Transport Theory and Statistical Physics 39 (2011) 73–109.

[9] E. Lewis, W. Miller, Computational Methods of Neutron Transport, John Wiley and Sons, New York, 1984.

[10] J. E. Morel, J. M. McGhee, E. W. Larsen, A Three-Dimensional Time-Dependent Unstructured Tetrahedral-Mesh SPN Method, Nuclear Science and Engineering 123 (1996) 1–9.

[11] J. A. Josef, J. E. Morel, Simplified spherical harmonic method for coupled electron-photon transport calculations, Physical Review E 57 (1998) 6161–6171.

[12] Y. Zhang, J. Ragusa, J. Morel, Iterative performance of various formulations of the SP_N equations, Journal of Computational Physics 252 (2013) 558–572.

[13] B. Adams, J. Morel, A two-grid acceleration scheme for the multigroup s_n equations with neutron upscattering, Nuclear Science and Engineering 115 (1993) 253–264.

[14] T. Evans, K. Clarno, J. Morel, A transport acceleration scheme for multigroup discrete ordinates with upscattering, Nuclear Science and Engineering 165 (3) (2010) 292–304.

[15] J. J. Duderstadt, L. J. Hamilton, Nuclear Reactor Analysis, John Wiley & Sons, 1976.

[16] K. S. Smith, Multidimensional nodal transport using the simplified p_l method, in: Proc. of Topical Conference on Reactor Physics and Safety, Saratoga Springs, NY, 1986, p. 223.

[17] V. Faber, T. Manteuffel, A look at transport theory from the point of view of linear algebra, in: P. Nelson, et al. (Eds.), Lecture Notes in Pure and Applied Mathematics, Vol. 115, Marcel Dekker, New York, 1988, pp. 31–61.

[18] G. Golub, C. van Loan, Matrix Computations, 3rd Edition, Johns Hopkins University Press, Baltimore, 1996.

[19] E. J. Allen, R. M. Berry, The inverse power method for calculation of multiplication factors, Annals of Nuclear Energy 29 (2002) 929–935.

[20] F. Scheben, I. G. Graham, Iterative methods for neutron transport eigenvalue problems, SIAM Journal on Scientific Computing 33 (2011) 2785–2804.

[21] S. Hamilton, Numerical solution of the k-eigenvalue problem, Ph.D. thesis, Emory University, Atlanta, GA (2011).

[22] R. N. Slaybaugh, T. M. Evans, G. G. Davidson, P. P. H. Wilson, Rayleigh quotient iteration in 3D, deterministic neutron transport, in: Advances in Reactor Physics Linking Research, Industry, and Education (PHYSOR 2012), Knoxville, TN, 2012.

[23] Y. Saad, Numerical Methods for Large Eigenvalue Problems, Manchester University Press, Manchester, UK, 1992.

[24] W. E. Arnoldi, The principle of minimized iterations in the solution of matrix eigenvalue problems, Quarterly of Applied Mathematics 9 (1951) 17–29.

[25] J. S. Warsa, T. A. Wareing, J. E. Morel, J. M. McGhee, R. B. Lehoucq, Krylov subspace iterations for deterministic k-eigenvalue calculation, Nuclear Science and Engineering 147 (2004) 26–42.

[26] G. G. Davidson, T. M. Evans, J. J. Jarrell, S. P. Hamilton, T. M. Pandya, R. N. Slaybaugh, Massively parallel, three-dimensional transport solutions for the k-eigenvalue problem, Nuclear Science and Engineering, forthcoming.

[27] E. R. Davidson, The iterative calculation of a few of the lowest eigenvalues and corresponding eigenvectors of large real-symmetric matrices, Journal of Computational Physics 17 (1975) 87–94.

[28] R. B. Morgan, D. S. Scott, Generalizations of Davidson's method for computing eigenvalues of sparse symmetric matrices, SIAM Journal on Scientific and Statistical Computing 7 (1986) 817–825.

[29] M. Sadkane, Block-Arnoldi and Davidson methods for unsymmetric large eigenvalue problems, Numerische Mathematik 64 (1993) 195–211.

[30] S. Hamilton, M. Benzi, A Davidson method for the k-eigenvalue problem, Transactions of the American Nuclear Society 105 (2011) 432–434.

[31] S. Subramanian, S. van Criekingen, V. Heuveline, F. Nataf, P. Havé, The Davidson method as an alternative to power iterations for criticality calculations, Annals of Nuclear Energy 38 (12) (2011) 2818–2823.

[32] G. L. G. Sleijpen, H. A. van der Vorst, A Jacobi–Davidson iteration method for linear eigenvalue problems, SIAM Journal on Matrix Analysis and Applications 17 (2) (1996) 401–425.

[33] D. Knoll, H. Park, C. Newman, Acceleration of k-eigenvalue/criticality calculations using the Jacobian-free Newton-Krylov method, Nuclear Science and Engineering 167 (2) (2011) 133–140.

[34] D. Gill, Y. Azmy, Newton's method for solving k-eigenvalue problems in neutron diffusion theory, Nuclear Science and Engineering 167 (2) (2011) 141–153.

[35] R. B. Morgan, Davidson's method and preconditioning for generalized eigenvalue problems, Journal of Computational Physics 89 (1990) 241–245.

[36] M. Crouzeix, B. Philippe, M. Sadkane, The Davidson method, SIAM Journal on Scientific Computing 15 (1994) 62–76.

[37] J. Olsen, P. Jorgensen, J. Simons, Passing the one-billion limit in full configuration-interaction (FCI) calculations, Chemical Physics Letters 169 (1990) 463–472.

[38] T. Evans, A. Stafford, R. Slaybaugh, K. Clarno, DENOVO: A new three-dimensional parallel discrete ordinates code in SCALE, Nuclear Technology 171 (2010) 171–200.

[39] M. Sala, M. Heroux, Robust algebraic preconditioners with IFPACK 3.0, Tech. Rep. SAND-0662, Sandia National Laboratories (2005).

[40] M. Gee, C. Siefert, J. Hu, R. Tuminaro, M. Sala, ML 5.0 smoothed aggregation user's guide, Tech. Rep. SAND2006-2649, Sandia National Laboratories, Albuquerque, NM (2006).

[41] R. N. Slaybaugh, T. M. Evans, G. G. Davidson, P. P. H. Wilson, Multigrid in energy preconditioner for Krylov solvers, Journal of Computational Physics 242 (2013) 405–419.

[42] E. Bavier, M. Hoemmen, S. Rajamanickam, H. Thornquist, Amesos2 and Belos: Direct and iterative solvers for large sparse linear systems, Scientific Programming 20 (3).

[43] Y. Saad, A flexible inner-outer preconditioned GMRES algorithm, SIAM Journal on Scientific Computing 14 (2) (1993) 461–469.

[44] M. A. Heroux, R. A. Bartlett, V. E. Howle, R. J. Hoekstra, J. J. Hu, T. G. Kolda, R. B. Lehoucq, K. R. Long, R. P. Pawlowski, E. T. Phipps, A. G. Salinger, H. K. Thornquist, R. S. Tuminaro, J. M. Willenbring, A. Williams, K. S. Stanley, An overview of the Trilinos project, ACM Trans. Math. Softw. 31 (3) (2005) 397–423. doi:http://doi.acm.org/10.1145/1089014.1089021.

[45] M. A. Smith, E. E. Lewis, B. C. Na, Benchmark on deterministic transport calculations without spatial homogenization – a 2-d/3-d mox fuel assembly benchmark (C5G7 MOX benchmark), Tech. Rep. NEA/NSC/DOC(2003)16, OECD/NEA (2003).

[46] E. E. Lewis, et al., Benchmark on deterministic calculations without spatial homogenization: MOX fuel assembly 3-D extension case, Tech. Rep. NEA/NSC/DOC(2005)16, OECD/NEA (2005).

[47] C. Cathalau, J. C. Lefebvre, J. P. West, Proposal for a second stage of the benchmark on power distributions within assemblies, Tech. Rep. NEA/NSC/DOC(96)2, Rev. 2, OECD/NEA (1996).

[48] SCALE: A comprehensive modeling and simulation suite for nuclear safety analysis and design, Tech. Rep. ORNL/TM-2005/39, Version 6.1, Oak Ridge National Laboratory, Oak Ridge, TN (2011).

[49] J. Gehin, A. Godfrey, F. Franceschini, T. Evans, B. Collins, S. Hamilton, Operational reactor model demonstration with VERA: Watts Bar Unit 1 cycle 1 zero power physics tests, Tech. Rep. CASL-U-2013-0105-001, Consortium for Advanced Simulation of LWRs (2013).

[50] M. Benzi, Preconditioning techniques for large linear systems: A survey, Journal of Computational Physics 182 (2002) 418–477.